



## Theoretical Study of the Electronic Characteristic of a TiO<sub>2</sub> -N719 Dye-Sensitized Solar Cell

Hadi J.M. Al-Agealy<sup>1\*</sup> , Hossain Milani Moghaddam<sup>2</sup>  and Mudhafar J. Ali<sup>3</sup> 

<sup>1</sup>Department of physics ,College of Education for Pure Science (Ibn-AL Haitham), University of Baghdad, Baghdad, Iraq.

<sup>2,3</sup>Department of Solid-State Physics, Faculty of Basic Sciences, University of Mazandaran, Babolsar, Iran.

\*Corresponding Author.

Received: 5 April 2023

Accepted: 8 May 2023

Published: 20 April 2024

[doi.org/10.30526/37.2.3381](https://doi.org/10.30526/37.2.3381)

### Abstract

A theoretical study of electronic characteristics based on charge transfer using quantum model N719 dye-sensitized contact with TiO<sub>2</sub> in solar cells. The current density expression used to calculate the photovoltaic characteristics is assumed to be a continuum level of the N719 dye and TiO<sub>2</sub> semiconductor in the heterojunction N719-TiO<sub>2</sub> devices using the MATLAB program. The transition energy, current, fill factor, and efficiency of N719-TiO<sub>2</sub> DSSCs are calculated based on quantum transition theory. The performance of DSSCs photovoltaic was estimated based on the I-V characteristics of the N719-TiO<sub>2</sub> device using concentrations ( $7 \times 10^{18} \text{ cm}^{-3}$ ) at (100 mW/cm<sup>2</sup>) irradiation. The N719-TiO<sub>2</sub> device with Butanol solvent at concentration ( $3 \times 10^{18} \text{ cm}^{-3}$ ) shows 0.8299 V, and (37.3034 mA/cm<sup>2</sup>) of open-circuit voltage and short-circuit current respectively fill factor of 0.206 compared to the open circuit of 0.8398 V and (87.5728 mA/cm<sup>2</sup>) and short-circuit current with fill factor of 0.257 at concentration of carrier ( $7 \times 10^{18} \text{ cm}^{-3}$ ). Current density and fill factor at limited transition energy increase with increasing the coupling constant and concentration of N719 - TiO<sub>2</sub> hetero junction and vice versa.

**Keywords:** Electronic Characteristic, TiO<sub>2</sub> -N719, Dye-Sensitized, Solar Cell.

### 1. Introduction

Concerns around climate change as a result of rising carbon dioxide levels in the atmosphere using fossil fuels and the increased demand for electricity due to an ever-growing population necessitate an effort to move away from the classical methods of energy production [1]. The necessity of switching to renewable energy to produce energy is urgent today. We can harness alternative sources for providing a sustainable and clean future using sunlight energy. Within this context, it is accessible, eco-friendly, and universal [2]. The photovoltaic solar cell has become more interested in energy research because it is a promised solution to the efficient conversion of solar energy. Additionally, more performance and device advancements are required to use this technology successfully in life [3]. The solar energy is one of the most sustainable and inexhaustible renewable sources that converts sunlight directly into electricity using solar cell devices without any pollutants [4]. Dye-sensitized solar cells, or "DSSCs," were begun after the work of Brian O'Regan and Michael Grätzel and have become a topic of interesting research for solar energy conversion because of their ease of



manufacture, low costs, eco-friendliness, and high conversion efficiency [5]. The dye-sensitized solar cells (DSSCs) are third-generation photo-electrochemical cells, and the photoactive electrodes are metal oxide and liquid-state electrolytes. In the last decade, DSSC has attracted considerably more interest because of its low-cost production, ease of process, and high photoelectrochemical performance [6].

TiO<sub>2</sub> is one of the oxide semiconductors with broadband gaps used as dye-adsorbed in the DSSCs technology that's renewed by the redox-coupled electrolyte solution [7]. The active medium usually consists of a donor state (organic solar cell) and an acceptor state (semiconductor) [8]. The basic reaction process in molecule contact with semiconductor electronic devices is the charge transfer reaction; electrons are moving between the donor state and the acceptor state [9]. The charge transfer is the main process in DSSCs that occurs in the solar cell system. Therefore, the transfer occurs under the assumed alignment of the energy levels of both the donor and acceptor states in DSSCs devices [10]. The N719 sensitized dye is widely used in DSSCs solar cells according to its many best characteristics, such as optical, electrochemical, synthesis, and photovoltaic properties [11]. In recent decades, charge transfer theory has been developed using different tools: analytical theory methods, time resolution, spectroscopy, and computer simulation [12].

Hadi et al. studied the charge transfer process in heterostructure devices according to the orientation energy under the alignment of energy states for materials in electronic devices. Electrons' move from one state to another is required to close energy levels in both materials [13]. The charge transfer in heterostructure devices depends on the orientation of the energy state in both the donor and acceptor states of contact [14]. DSSCs contain a sensitizer dye that absorbs sunlight to excite, and electrons are moved into the conduction band of TiO<sub>2</sub>. In general, the ruthenium N719 sensitizer dye has the best electronic stability and transportability to be used in DSSCs [15]. More TiO<sub>2</sub> is being used as a photoanode for DSSC because it has a large surface area, is chemically stable, has large catalyst band edges, is not toxic, and has low recombination [16]. In recent years, the development of device structures, redox mediators, and sensitizers has improved the performance of DSSCs [17].

Di-tetrabutylammonium, cis-bis (isothiocyanato) bis (2,2'-bipyridyl-dicarboxylato 4,4') Ruthenium(II) sensitizers are one of the appropriate sensitizer molecules with DSSCs [18]. **Figure 1**, illustrates the chemical structure of N719 [19]. In this work, the electronic characteristics of the N719-TiO<sub>2</sub> heterojunction have been studied theoretically based on transition theory according to the quantum model.

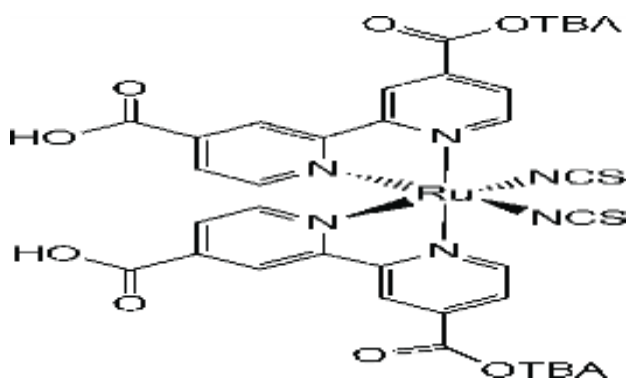


**Figure 1.** Structure of N719 sensitised dye [19]

## 2. Theory

The probability of charge transfer per unit time from one state to another state in hetero-junction

may be given as [20].

$$T_D^A(E) = \sum \frac{4\pi^2}{h} |\langle H_C \rangle|^2 \rho_{ac}(E) \quad (1)$$

Where  $h$  is Planck constant,  $H_C$  is the coupling constant between materials in hetro junction and  $\rho_{ac}(E)$  is activation density,  $\rho_{ac}(E)$  is given by [21].

$$\rho_{ac}(E) = D_S \frac{l_{ac}}{\left(\frac{6}{\pi}\right)^{1/3}} \quad (2)$$

where  $D_S$  the density of states at room temperature is,  $l_{ac}$  is the activated length .The density of states for

the charge transfer can be written as [22]

$$D_S = D_d(E) \langle \hat{\rho} \rangle d_s^{-2/3} \quad (3)$$

where  $D_d(E)$  is density of charge in dye,  $\langle \hat{\rho} \rangle$  is the density of state in a system,  $d_s$  is the atomic density in semiconductor. The density of state in a system  $\langle \hat{\rho} \rangle$  is [23].

$$\langle \hat{\rho} \rangle = \frac{1}{\sqrt{4\pi\Lambda_S^M k_B T}} e^{-\frac{(\Lambda_S^M + \Delta F^0)^2}{4\Lambda_S^M k_B T}} \quad (4)$$

where  $\Delta F^0$  is driving energy,  $k_B$  is Boltzman constant ,T is room temperature, and  $\Lambda_S^M$  is the transition energy .The driving energy  $\Delta F^0$  is given by[24].

$$\Delta F^0 = (E_c q E_o) \quad (5)$$

where  $E_c$  is conduction band of TiO2 and  $q E_o$  is chemical potential of dye . Inserting **Eqs** (4),(3) and (2) in **Eqs** (1) to obtain .

$$T_D^A(E) = \sum \frac{4\pi^2}{h} |\langle H_C \rangle|^2 D_d(E) \frac{1}{\sqrt{4\pi\Lambda_S^M k_B T}} e^{-\frac{(\Lambda_S^M + \Delta F^0)^2}{4\Lambda_S^M k_B T}} d_s^{-2/3} \frac{l_{ac}}{\left(\frac{6}{\pi}\right)^{1/3}}. \quad (6)$$

The current of charge through system is [25].

$$I = e \sum F(E) T_D^A(E) \quad (7)$$

where  $F(E)$  is Fermi distribution in system. Inserting Eq.(6) in Eq.(7) and integrate to result.

$$I = \frac{4\pi^2}{h} |\langle H_C \rangle|^2 \frac{1}{\sqrt{4\pi\Lambda_S^M k_B T}} e^{-\frac{(\Lambda + \Delta F^0)^2}{4\Lambda k_B T}} d_s^{-2/3} \frac{l_{ac}}{\left(\frac{6}{\pi}\right)^{1/3}} \int_0^{qE} D_d(E) F(E) dE \quad (8)$$

Integral in **Equations** 8 over chemical potential of dye is reduced to concentration of dye  $[n]$  [26]

$$\int_0^{qE} D_d(E) F(E) dE = [n] \quad (9)$$

The current expression in Eq.(8) with Eq.(8) is reduced to:

$$I(mA) = \frac{4\pi^2}{h} [n] |\langle H_C \rangle|^2 \frac{1}{\sqrt{4\pi\Lambda_S^M k_B T}} e^{-\frac{(\Lambda + \Delta F^0)^2}{4\Lambda k_B T}} d_s^{-2/3} \frac{l_{ac}}{\left(\frac{6}{\pi}\right)^{1/3}} \quad (10)$$

The atomic density of semiconductor  $d_s$  is estimated using the number of states  $N_s$  and density of states  $D_s$  and is written as [27].

$$d_s = \frac{N_s}{D_s} \quad (11)$$

The density of states  $D_s$  of semiconductor is estimated using formula [27].

$$D_s = \frac{3}{2} \left( \frac{N_e}{E_F} \right) \quad (12)$$

where  $N_e$  is carrier concentration and  $E_F$  is Fermi energy of semiconductor. The current density is given by ratio of current divided on area and given by

$$I \left( \frac{mA}{cm^2} \right) = \frac{I(mA)}{Area} \quad (13)$$

The fill factor is ratio relative to I-V curve's maximum power is unit less, it describes to the maximum power  $J_m V_m$ . and give ratio [28].

$$FF = \frac{J_m V_m}{J_{sc} V_{oc}} \quad (14)$$

where  $I_{sc}$  is short-circuit current, and  $V_{oc}$  is open circuit voltages. Transition energy for charge transfer from one state to another state is [29].

$$\Lambda_{AD}(eV) = \frac{e^2}{8\pi\epsilon_0} \left[ \frac{1}{D} \Lambda(n, \epsilon) - \frac{1}{2R} [\Lambda(n_{sem}, n) - \Lambda(\epsilon_{sem}, \epsilon)] \right] \quad (15)$$

Where  $e$  and  $\epsilon_0$  are electric charge and vacuum permittivity,  $D$  and  $R$  are the radius dye and distance between the complex and the semiconductor, respectively,  $\Lambda(n, \epsilon) = \left[ \frac{1}{n^2} - \frac{1}{\epsilon} \right]$  is the polarity solvent as function of refractive index  $n$  and dielectric constant  $\epsilon$  of solvent,  $\Lambda(n_{sem}, n) = \left[ \frac{n_{sem}^2 - n^2}{n_{sem}^2 + n^2} \right] \left( \frac{1}{n^2} \right)$  is an optical dielectric for semiconductor - solvent term where  $n_{sem}$  is refractive index of semiconductor and  $\Lambda(\epsilon_{sem}, \epsilon) = \left[ \frac{\epsilon_{sem}^2 - \epsilon^2}{\epsilon_{sem}^2 + \epsilon^2} \right] \frac{1}{\epsilon^2}$  is statical dielectric term where  $\epsilon_{sem}$  is dielectric constant of the semiconductor. The radii of atom and molecule evaluate according to apparent molar volumes approach [30].

$$D(m) = \left( \frac{3}{4\pi} \frac{M}{N\rho} \right)^{\frac{1}{3}} \quad (16)$$

where  $M$  is the m

olecular weight,  $N$  is the Avogadro number, and  $\rho$  is the density of material.

### 3. Results and discussion

The electronic characteristic of TiO<sub>2</sub>-N719 hetero junction is investigated based on a theoretical model for charge transfer in DSSCs solar cell. We estimate the transition energy, current, atomic density, density of states, current density, and fill factor according to a simple theoretical scenario. In general, the electronic characteristics of N719-TiO<sub>2</sub> devices were calculated theoretically by a MATLAB program as a function of transition energy  $\Lambda_S^M$  (eV in Eq. (15)). Firstly, we calculate the radii of N719 and TiO<sub>2</sub> according to the continuum model. In essence, the radii of both N719 dye and TiO<sub>2</sub> are estimated using Eq.(16) by taking the molecular weight and density,  $M= 1188.55\text{g/mol}$ ; the density  $\rho = 1.52 \frac{\text{g}}{\text{cm}^3}$  for N719 dye and  $M=79.866\text{g/mol}$  and  $\rho = 4.23 \frac{\text{g}}{\text{cm}^3}$  for TiO<sub>2</sub>[31], results of the radii of N719 and TiO<sub>2</sub> are  $6.769 \text{ \AA}$  and  $1.956 \text{ \AA}$ , respectively. Transition energy is calculated using Eq. (16) by inserting the parameters  $n=1.3993$  and  $\epsilon = 17.51$  of 1-Butanol [32],  $n_s = 2.609$  [31] and  $\epsilon_s = 55$  for TiO<sub>2</sub>,  $D = 6.769 \text{ \AA}$ ,  $R=8.725 \text{ \AA}$  to result  $\Lambda_S^M = 0.367\text{eV}$ . It shows that the N719-TiO<sub>2</sub> system needs  $0.367\text{eV}$  to start transferring from excited levels of dye to the conduction band in the TiO<sub>2</sub> semiconductor. The density of states of the  $D_s$  of TiO<sub>2</sub> semiconductor is calculated by inserting the carrier concentration  $N_e = 1.4 \times 10^{14} \frac{1}{\text{cm}^3}$  [33] and Fermi energy  $E_F = 4.19\text{eV}$  [34]

in Eq. (12) to give  $D_s = 3.34 \times 10^{13} \frac{\text{electron}}{\text{cm}^3 \cdot \text{eV}}$ . The atomic density in Eq. (11) was estimated using  $N_s = 8 \frac{\text{electron}}{\text{eV}}$  and  $D_s = 3.34 \times 10^{13} \frac{\text{electron}}{\text{cm}^3 \cdot \text{eV}}$  [32] to result  $d_s = 4.1766 \times 10^{18} \frac{1}{\text{m}^3}$ . The electronic current of N719-TiO<sub>2</sub> solar cell with 1-Butanol solvent is calculated using Eq.(10) which takes  $|(H_C)|^2=0.15,0.25,0.35,0.45,0.55,0.65,0.75,0.85, 0.95,1.05,1.15,1.25,1.35,1.45$  and  $1.55 \times 10^{-2} \text{eV}^2, \Lambda_S^M = 0.339 \text{ eV}, l_{ac} = 3A^0, d_s = 4.17 \times 10^{18} \frac{1}{\text{m}^3}, [n] = (3 \text{ and } 7) \times 10^{24} \frac{1}{\text{m}^3}$  [35], results are listed in **Table 1**.

**Table 1.** Results of electronic current calculation for N749/TiO<sub>2</sub> with 1-Butanol solvent

| Strength coupling  eV/ state  <sup>2</sup><br> (C <sub>CET</sub> )  <sup>2</sup> × 10 <sup>-2</sup> | The electronic current                      |   |
|---|---|---|
|   | The electronic concentration                |   |
|   | 3 × 10 <sup>24</sup> $\frac{1}{\text{m}^3}$ | 7 × 10 <sup>24</sup> $\frac{1}{\text{m}^3}$ |
| 0.15  | 1.6666E-03                                  | 3.8888E-03                                  |
| 0.25  | 2.7777E-03                                  | 6.4814E-03                                  |
| 0.35  | 3.8888E-03                                  | 9.0739E-03                                  |
| 0.45  | 4.9999E-03                                  | 1.1666E-02                                  |
| 0.55  | 6.1110E-03                                  | 1.4259E-02                                  |
| 0.65  | 7.2221E-03                                  | 1.6852E-02                                  |
| 0.75  | 8.3332E-03                                  | 1.9444E-02                                  |
| 0.85  | 9.4443E-03                                  | 2.2037E-02                                  |
| 0.95  | 1.0555E-02                                  | 2.4629E-02                                  |
| 1.05  | 1.1666E-02                                  | 2.7222E-02                                  |
| 1.15  | 1.2778E-02                                  | 2.9814E-02                                  |
| 1.25  | 1.3889E-02                                  | 3.2407E-02                                  |
| 1.35  | 1.5000E-02                                  | 3.4999E-02                                  |
| 1.45  | 1.6111E-02                                  | 3.7592E-02                                  |
| 1.55  | 1.7222E-02                                  | 4.0185E-02                                  |

The current in **Table 1**, indicates that it depends on the concentration and coupling constant between N719 dye and TiO<sub>2</sub> in a solar cell system. It can be seen that the current is increased upon increasing the coupling between N719 and TiO<sub>2</sub> and increasing the concentration. However, the current density is calculated according to Eq. (13) by taking the results from Table 1 and dividing by the area of the cell (0.49 cm<sup>2</sup>) [36]. The results are shown in **Table 2**.

**Table 2.** Results of current density for N749/TiO<sub>2</sub> with 1-Butanol

| Strength coupling  eV/ state  <sup>2</sup><br> (C <sub>CET</sub> )  <sup>2</sup> × 10 <sup>-2</sup> | The current density ( $\frac{\text{mA}}{\text{cm}^2}$ ) |  |
|---|---|--|
|   | The electronic concentration                            |  |
|   | 3 × 10 <sup>18</sup> $\frac{1}{\text{cm}^3}$            | 7 × 10 <sup>18</sup> $\frac{1}{\text{cm}^3}$ |
| 0.15  | 3.40122   | 7.9363                                       |
| 0.25  | 5.6687  | 13.2273                                      |
| 0.35  | 7.99363   | 18.51816                                     |
| 0.45  | 10.2038   | 23.80816                                     |
| 0.55  | 12.4714   | 29.1   |
| 0.65  | 14.7387   | 34.3918                                      |
| 0.75  | 17.0065   | 39.6816                                      |
| 0.85  | 19.2747   | 44.97346                                     |
| 0.95  | 21.54081  | 50.26326                                     |
| 1.05  | 23.80816  | 55.5551                                      |

|      |           |           |
|------|-----------|-----------|
| 1.15 | 26.07755  | 60.84489  |
| 1.25 | 28.344898 | 136766.   |
| 1.35 | 30.61224  | 71.4265   |
| 1.45 | 32.87959  | 76.7183   |
| 1.55 |           | 35.1469   |
|      |           | 82.201020 |

Both current and current density in **Tables 1** and **2**, are increased with increasing in the coupling of energy levels for dye and TiO<sub>2</sub> in the system from  $0.150 \times 10^{-2} \text{ |eV/ state|^2}$  to  $1.550 \times 10^{-2} \text{ |eV/ state|^2}$ . However, the current density in **Table 2**, increases with increasing the carrier concentration with 1-butanol solvent media in the system devices. In turn, the current density is affected by the fill factor and J-V characteristics of the cell. As it can be seen, the current density increases with an increasing the concentration from  $3 \times 10^{18} \frac{1}{\text{cm}^3}$  to  $7 \times 10^{18} \frac{1}{\text{cm}^3}$  by a percentage 2.33. This means more electrons are transferred with increasing the carrier cross-interface of N719 dye contact with the TiO<sub>2</sub> hetero junction. Additionally, the concentration, coupling constant, and current density limit the electronic properties of N719-TiO<sub>2</sub>. The current density increases with increasing the coupling for concentrations in cell system. The photovoltaic J-V results of current density J (mA/cm<sup>2</sup>) and voltage in Volt for the N719 - TiO<sub>2</sub> DSSCs using theoretical methods are shown in **Table 3**.

**Table 3.** The photovoltaic J-V results for N719/TiO<sub>2</sub> with 1-Butano

| The electronic concentration             |   |  |   |  |
|--|---|--|---|--|
| $3 \times 10^{18} \frac{1}{\text{cm}^3}$ |   | $7 \times 10^{18} \frac{1}{\text{cm}^3}$ |   |  |
| V (volt)                                 | $J(E) \left( \frac{\text{mA}}{\text{cm}^2} \right)$ | V (volt)                                 | $J(E) \left( \frac{\text{mA}}{\text{cm}^2} \right)$ |  |
| 0.8299                                   | 0   | 0.8398                                   | 0   |  |
| 0.8                                      | 3.40122   | 0.8                                      | 7.9363  |  |
| 0.75                                     | 5.6687  | 0.75                                     | 13.2273   |  |
| 0.7                                      | 7.99363   | 0.7                                      | 18.51816  |  |
| 0.65                                     | 10.2038   | 0.65                                     | 23.80816  |  |
| 0.6                                      | 12.4714   | 0.6                                      | 29.1  |  |
| 0.55                                     | 14.7387   | 0.55                                     | 34.3918   |  |
| 0.5                                      | 17.0065   | 0.5                                      | 39.6816   |  |
| 0.45                                     | 19.2747   | 0.45                                     | 44.97346  |  |
| 0.4                                      | 21.54081  | 0.4                                      | 50.26326  |  |
| 0.35                                     | 23,80816  | 0.35                                     | 55.5551   |  |
| 0.3                                      | 26.07755  | 0.3                                      | 60.84489  |  |
| 0.25                                     | 28.344898   | 0.25                                     | 136766.   |  |
| 0.2                                      | 30.61224  | 0.2                                      | 71.4265   |  |
| 0.15                                     | 32.87959  | 0.15                                     | 76.7183   |  |
| 0.1                                      | 35.1469   | 0.1                                      | 82.201020   |  |
| 0  | 37.3034   | 0  | 87.5728   |  |

The J-V characteristics are plotted in **Figure 1**, with two concentrations. Depending on the two curves in **Figures 1** and **2** the average current and voltage in the open circuit can be limited, and the results are listed in Table 4 for both concentrations. Furthermore, the fill factor can be estimated using Eq.(14) under simulated AM 1.5 global sunlight (1 Sun, 100 mW/cm<sup>2</sup>) by using data of average current and voltage in the open circuit from the curves in **Figure 1**. The results are shown in **Table 4**, for both concentrations of 1-butanol solvent.

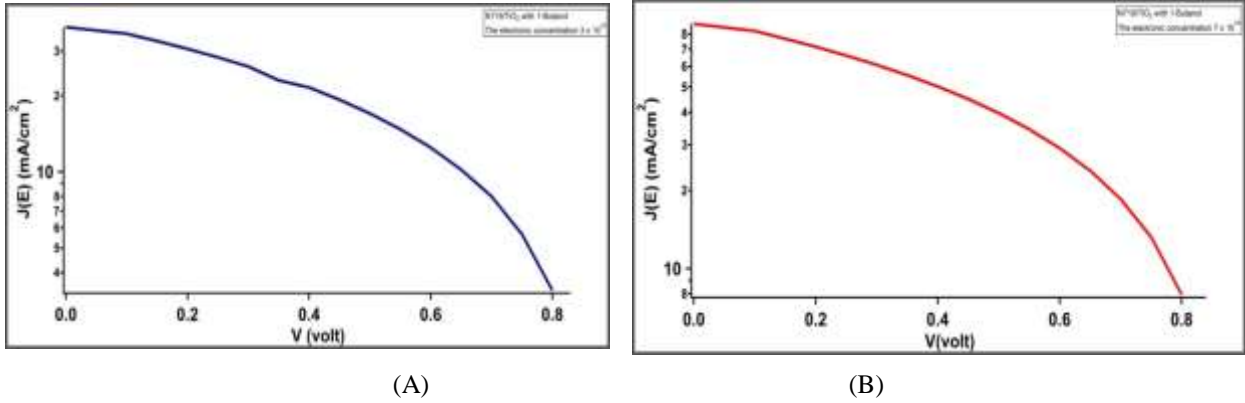


**Figure 1.** The J-V curves with concentration carrier A)  $3 \times 10^{18} \frac{1}{cm^3}$  and B)  $7 \times 10^{18} \frac{1}{cm^3}$  of the N719-TiO<sub>2</sub> devices

**Table 4.** Photovoltaic parameters of the N719-TiO<sub>2</sub> DSSCs employing two different types of concentration carriers

| Variables         | The electronic concentration 1/cm <sup>3</sup> |                    |
|-------------------|--|--------------------|
|                   | $3 \times 10^{18}$                             | $7 \times 10^{18}$ |
| $J_{Sc}(mA/cm^2)$ | 37.3034  | 87.5728            |
| $V_{oc}$ Volt     | 0.8299   | 0.8398             |
| $J_m(mA/cm^2)$    | 32.755   | 61.010             |
| $V_m$ Volt        | 0.195  | 0.31               |
| F.F               | 0.206  | 0.257              |

As it can be seen, the fill factor increases with increasing the concentration from  $3 \times 10^{18} 1/cm^3$  to  $7 \times 10^{18} 1/cm^3$ . **Table 4**, shows that the average current  $J_m$  is 32.755 mA/cm<sup>2</sup> and voltage  $V_m$  is 0.195V in open-circuit where the current  $J_{Sc}$  is 37.3034 mA/cm<sup>2</sup> and the voltage  $V_{oc}$  is 0.8299 V in open circuit. The fill factor FF = 0.206 of N719-TiO<sub>2</sub> DSSC with concentration  $3 \times 10^{18} cm^{-3}$ . On the other hand, the average current  $J_m$  is 61.010 mA/cm<sup>2</sup> and the voltage  $V_m$  is 0.31V in open-circuit where the current  $I_{Sc}$  is 87.5728 mA/cm<sup>2</sup> and voltage  $V_{oc}$  is 0.8398V in open circuit and that the cell achieved a FF = 0.257 at concentration  $7 \times 10^{18} cm^{-3}$ . However,  $J_{Sc}$  (87.5728 mAcm<sup>-2</sup>) at concentration  $7 \times 10^{18} cm^{-3}$  was relatively higher than  $J_{Sc}$  (37.3034 mAcm<sup>-2</sup>) at concentration  $3 \times 10^{18} cm^{-3}$  and the  $V_{oc}$  (0.8398V) at  $7 \times 10^{18} cm^{-3}$  was almost the same to the  $V_{oc}$  (0.8299V) at concentration  $3 \times 10^{18} cm^{-3}$  offered by the TiO<sub>2</sub> electrode. However, the increased increasing the carrier concentration results in increasing the current density and fill factor.

#### 4. Conclusion

The electronic characteristics of the N719-TiO<sub>2</sub> device are investigated and studied using a simple transition model for charge transfer using two different concentrations of carriers. The butanol solvent was an active media for the N719-TiO<sub>2</sub> solar cell due to the transition energy that's affected by the

current density and fill factor parameters. Current, current density, and fill factor are strongly influenced by concentration and coupling constants with limited transition energy. Increasing both coupling strength and concentration at limited transition energy reduced increased transfer through N719-TiO<sub>2</sub> devices and affected the J-V characteristic and fill factor of the solar cell. The (61.010 mA/ Cm<sup>2</sup>) and (0.31 Volt) exhibit large values of FF (0.286) at a carrier concentration of about  $3 \times 10^{18} \frac{1}{cm^3}$ , which helps in understanding the performance device.

### **Acknowledgement**

I extend my thanks to the College of Education for pure science Ibn Al-Haitham, University of Baghdad for assisting in completing this work by opening private laboratories and providing scientific facilities by the staff of the Physics Department to help support the research project.

### **Conflict of Interest**

The authors declare that they have no conflicts of interest.

**Funding:** None.

### **References**

1. Wilson, G. M.; Al-Jassim, M; Metzger, W. K.; Glunz, S. W.; Verlinden, P.; Xiong, G.; Mansfield, L. M.; Stanbery, B. J.; Zhu, K.; Yan, Y. The photovoltaic technologies roadmap, *J. Phys. D Appl. Phys* **2020**, *53*, 493001. <https://doi.org/10.1088/1361-6463%2F53%2F493001>
2. Muhammad, J. Y. U.; Waziri, A. B.; Shitu, A. M.; Ahmad, U. M.; Muhammad, M. H.; Alhaji, Y.; Olaniyi, A. T.; Bala, A. A. Recent progressive status of materials for solar photovoltaic cell: A comprehensive review. *Sci. J. Energy Eng* **2019**, *7*, 77–89. <https://doi.org/10.11648/J.SJEE.20190704.14>
3. Moorthy, V. M.; Srivastava, V. M.; Device Modelling and Optimization of Nanomaterial-Based Planar Heterojunction Solar Cell (by Varying the Device Dimensions and Material Parameters, *Nanomaterials*. **2022**, *12*, 3031. <https://doi.org/10.3390/nano12173031>
4. Aga, F. G.; Bakare, F. F.; Dibaba, S. T.; Gelmecha, D. J.; Amente, C. Investigation of the Impact of Active Layer and Charge Transfer Layer Materials on the Performance of Polymer Solar Cells through Simulation, *Advances in Materials Science and Engineering* **2022**, <https://doi.org/10.1155/2022%2F6779260> .
5. Naeem, N. A.; Al-Agealy, H. J. M.; Hossain, M. M. Theoretical Calculation of The Fill Factor of N749/TiO<sub>2</sub> Solar Cells, *IHJPAS* **2023**, *36(4)*, 12-23. <http://dx.doi.org/10.1063/5.0172672>
6. Seung, M. L.; Juyoung, M.; Uoon, C. B.; Jae, Y. L.; Youngjin, C.; Jung, T. P.; Shape-Controlled TiO<sub>2</sub> Nanomaterials-Based Hybrid Solid-State Electrolytes for Solar Energy Conversion with a Mesoporous Carbon Electrocatalyst, *Nanomaterials* **2021**, *11*, 913. <https://doi.org/10.1016/j.jpowsour.2021.230429>
7. Estabraq, H. R.; Hadi, J. M. A. A Theoretical Investigation of Charge Transfer Dynamics from Sensitized Molecule D35CPDT Dye to SnO<sub>2</sub> and TiO<sub>2</sub> Semiconductor, *IHJPAS* **2022**, *53(3)*, 23-34. <https://doi.org/10.1063/5.0092689>
8. Wang, Q.; Zeng, Z.; Li, Y.; Chen, X. Efficient strategies for improving the performance of EDOT derivatives and TPA derivatives-based hole transport materials for perovskite solar cells, *Solar Energy* **2020**, *208(15)*, 10-19. <https://doi.org/10.1002/anie.202116068>
9. Hadi, J. M. A.; Alshafaay, B.; Mohsin, A. H.; Ahmed, A.; Abbas, K. S.; Raad, H. M.; Rawnaq, Q. G.; Shatha, H. M. Theoretical Discussion of Electron Transport Rate Constant TCNQ / Ge and TiO<sub>2</sub> System. *IOP Conf. Series: Journal of Physics: Conf. Series* **2018**, *1003*, 012122. <http://dx.doi.org/10.1088/1742-6596/1003/1/012122>

10. Li, X.; Zhang, Q.; Yu, J.; Xu, Y.; Zhang, R.; Wang, C.; Zhan, H.; Fabiano, S.; Liu, X.; Hou, J.; Gao, F.; Fahlman, M. Mapping the energy level alignment at donor/acceptor interfaces in non-fullerene organic solar cells. *Nature Communications* **2022**, *13*(1), 20-46. <https://doi.org/10.1016/j.joule.2020.02.014>
11. Maysari, H. L. Enhanced performance of dye sensitized solar cells using melinjo peel (Gnetum gnemon) dye as sensitizer, *Indonesian Physical Review* **2019**, *3*, 106-115. <http://dx.doi.org/10.29303/ipr.v2i3.28>
12. Hadi, J. M.; Khaled, H. H.; Mohsin, A. H.; Rafah, I. N. Theoretical Study of Charge Transfer in Styryl Thiazilo Quinoxaline Dyes STQ-1, STQ-2, and STQ-3 in Organic Media System. *Baghdad Science Journal* **2013**, *10*(4), 214-219. <http://dx.doi.org/10.1016/j.egypro.2017.07.116>
13. Hadi, J. M. A.; Hassoni, M. A. H.; Ahmad, M. S.; Noori, R. I.; Jheil, S. S. Theoretical Study of Charge Transport at Au/ZnSe and Au/ZnS Interfaces Devices. *Ibn AL-Haitham J. Pure and Appl. Sci* **2017**, *27*(1), 176-187. <http://dx.doi.org/10.1063/5.0129535/16940584/020035>
14. Hadi, J. M. A.; Hassooni, M. A. Calculate of the Rate Constant of Electron Transfer in TiO<sub>2</sub>-Safranin Dye System, *Ibn AL-Haitham J. Pure and Appl. Sci* **2017**, *24*(3), 22-34.
15. Jayachithra, J. V.; Elampari, K.; Meena, M. Fabrication of TiO<sub>2</sub> based Dye-Sensitized Solar Cell using Nerium oleander as a sensitizer, *IOP Conf. Series: Materials Science and Engineering*. **2022**, *1263*. <https://doi.org/10.1088/1757-899X/2F1263/2F1%2F012018>
16. Gnida, P.; Jarka, P.; Chulkin, P.; Drygała, A.; Libera, M.; Nsk, T. T.; Schab-Balcerzak, E. Impact of TiO<sub>2</sub> Nanostructures on Dye-Sensitized Solar Cells Performance, *Sci. Materials* **2021**, *14*, 1633. <https://doi.org/10.3390/ma14071633>
17. Ren, Y.; Zhang, D.; Suo, J.; Cao, Y.; Eickemeyer, F. T.; Vlachopoulos, N.; Zakeeruddin, S. M.; Hagfeldt, A.;ätzel, M. I. Hydroxamic acid pre-adsorption raises the efficiency of cosensitized solar cells, *Nature of science* **2023**, *613*, 60-65. <https://doi.org/10.1038/s41586-022-05460-z>
18. Roya, A.; Mohamed, M. J. S.; Gondalb, M. A.; Mallick, T. K.; Tahira, A. A.; Sundaramd, S.; Co-sensitization effect of N719 dye with Cu doped CdS colloidal nanoparticles for dye-sensitized solar cells, *Inorganic Chemistry Communications. Appl. Phys* **2023**, *148*, 110298. <https://doi.org/10.1002/er.4288>
19. Cortez, K. P.; Martínez, A.; Dutt, A.; Santana, G.; N719 Derivatives for Application in a Dye-Sensitized Solar Cell (DSSC): A Theoretical Study, *J. Phys. Chem. A* **2019**, *123*(51), 10930-1093. <https://doi.org/10.1021/acs.jpca.9b09024>
20. Taif, S. A.; Jumali, M. H.; Hadi, J. M.; Abdul Razak, F. B.; Yap, C. C. An Investigation of the Fill Factor and Efficiency of Molecular Semiconductor Solar Cells, *Materials Science Forum* Submitted **2021**, *1039*, 373-381. <http://dx.doi.org/10.1140/epjp/s13360-023-03935-0>
21. Taif, S. A.; Hadi, J. M.; Zahraa, H. M.; Bahjat, B. K.; Hiba, A. M. Charge Transfer from Indoline Dye Contact to Zinc Selenide: Analytical, *International Journal of Mechanical Engineering* **2022**, *7*(2), 3-12.
22. Al-Obaidi, S. S.; Hadi, J. M.; Abbas, S. R. Theoretical Evaluation of Flow Electronic Rate at Au /TFB Interface, *Journal of Physics: Conference Series* **2021**, 1879.
23. Hadi, J. M.; Sarmad, S. A.; Saadi, R. A. Theoretical Study and Calculation of Electronic Current Flow at Platinum Metal Contact with TFP Molecule Systems, *AIP Conference Proceedings*. **2022**, 2398, 020024. <http://dx.doi.org/10.4028/p-8EdAER>
24. Methaq, A. R.; Hadi, J. M. Theoretical calculation of the electronic current at N3 contact with TiO<sub>2</sub> solar cell devices, *AIP Conference Proceedings* **2022**, 2437, 020060. <http://dx.doi.org/10.1063/5.0092690>
25. Derosa, P. A.; Seminario, J. M. Electron Transport through Single Molecules: Scattering Treatment Using Density Functional and Green Function Theories, *J. Phys. Chem. B* **2001**, *105*, 471-481. <https://doi.org/10.1021/JP003033%2B>
26. Methaq, A. R.; Hadi, J. M. Theoretical investigation of charge transfer at N3 sensitized molecule dye contact with TiO<sub>2</sub> and ZnO semiconductor, *AIP Conference Proceedings* **2022**, 2437, 020059.
27. Royea, W. J.; Fajardo, A. M.; Lewis, N. S. Fermi Golden Rule Approach to Evaluating Outer-Sphere Electron-Transfer Rate Constants at Semiconductor/Liquid Interfaces, *J. Phys. Chem. B* **1997**, *101*, 11152-11159. <https://doi.org/10.1126/science.274.5289.969>

28. Khatibi, A.; Astaraei, F. R.; Ahmadi, M. H.; Generation and combination of the solar cells: A current model review, *Energy Sci. Eng* **2019**, *23*, 1–18. <https://doi.org/10.1002/ese3.292>
29. Hadi, J. A.; Mohammad, Z. Fa. Estimation of the Electric Properties of Al/Cv System. *Journal of University of Babylon for Pure and Applied Sciences* **2020**, *12(33)*, 184-193. <https://doi.org/10.1063/1.5132985>
30. Hadi, J. A.; Hassoni, M. A. A theoretical study of the effect of the solvent type on the reorganization energies of dye /semiconductor system interface. *Ibn-Al Haithem .J for pure & Appl. Sci* **2010**, *23(3)*, 51-57. <http://dx.doi.org/10.30526/36.4.3382>
31. Abbas, K. S.; Hadi, J. M. Study of photoemission and electronic properties of dye-sensitized solar cells, *Energy Reports* **2020**, *6*, 3, 28-35. <http://dx.doi.org/10.1016/j.egy.2019.10.015>
32. Haynes, W. M.; Handbook of Chemistry and Physics, First Eds., *Imprint CRC Press Publ* **2014**, *12*, 233-245. <https://doi.org/10.1201/9781315380476>
33. Lin, Y. J.; Yang, S. H.; Carrier transport and photoresponse for heterojunction diodes based on the reduced graphene oxide-based TiO<sub>2</sub> composite and p-type Si . *Appl. Phys. A* **2014**, *116*, 91–95.
34. Xu, Z.; Wu, J.; Wu, T.; Bao, Q.; He, X.; Lan, Z.; Lin, J.; Huang, M.; Huang, Y.; Fan, L. Tuning the Fermi Level of TiO<sub>2</sub> Electron Transport Layer through Europium Doping for Highly Efficient Perovskite Solar Cells. *Energy Technol* **2017**, *5*, 1820–1826. <http://dx.doi.org/10.1007/s40820-023-01087-5>
35. Tahir, M.; Din, I.; Zeb, M.; Aziz, F.; Wahab, F.; Gul, Z.; Sarker, M. R.; Ali, S.; Ali, S. H. Kymissis, I.; Thin Films Characterization and Study of N749-Black Dye for Photovoltaic Applications. *Coatings* **2022**, *12*, 1163 .
36. Gnida, P.; Jarka, P.; Chulkin, P.; Drygała, A.; Libera, M.; Tnski, T.; Balcerzak, E. S. Impact of TiO<sub>2</sub> Nanostructures on Dye-Sensitized Solar Cells Performance tert-Butyl alcohol (CH<sub>3</sub>)<sub>3</sub>COH. *Journal of Materials* **2021**, *14*, 1633. <https://doi.org/10.3390/ma14071633>